available at www.sciencedirect.comwww.elsevier.com/locate/brainres
**BRAIN
RESEARCH**

Research Report

Integration of force and position cues for shape perception through active touch

Knut Drewing*, Marc O. Ernst

Max Planck Institute for Biological Cybernetics, Tübingen, Germany

ARTICLE INFO

Article history:

Accepted 9 December 2005

Available online 21 February 2006

Keywords:

Cue integration

Active touch

Psychophysics

Haptic perception

Human

ABSTRACT

This article systematically explores cue integration within active touch. Our research builds upon a recently made distinction between position and force cues for haptic shape perception [Robles-de-la-Torre, G., Hayward, V., 2001. Force can overcome object geometry in the perception of shape through active touch, *Nature* 412, 445–448]: when sliding a finger across a bumpy surface, the finger follows the surface geometry (position cue). At the same time, the finger is exposed to forces related to the slope of the surface (force cue). Experiment 1 independently varied force and position cues to the curvature of 3D arches. Perceived curvature could be well described as a weighted average of the two cues. Experiment 2 found more weight of the position cue for more convex high arches and higher weight of the force cue for less convex shallow arches—probably mediated through a change in relative cue reliability. Both findings are in good agreement with the maximum-likelihood estimation (MLE) model for cue integration and, thus, carry this model over to the domain of active haptic perception.

© 2005 Elsevier B.V. All rights reserved.

1. Introduction

Perception is based on multiple sources of sensory information—we simultaneously and continuously obtain sensory inputs from our eyes, ears, and the skin. Imagine holding a black purring cat. We obtain inputs that complement one another, when we see the cat's size, its color, and hear what sounds it produces. Some of the inputs provide information about the same physical property. We can both see and feel the size of the cat. The question of how our brain integrates such redundant cues into a unitary percept has been studied intensively in the recent past. Several models of cue integration have been suggested (for reviews, Bühlhoff and Mallot, 1988; Howard and Rogers, 2002).

The maximum-likelihood estimation (MLE) model has been proven to be a good description for cue integration strategies (Ernst and Bühlhoff, 2004). According to this model, the brain takes into account all cues available for a property, derives estimates (s_i) for the property from each cue (i), and then combines all these estimates into a coherent percept (P) by weighted averaging:

$$P = \sum_i w_i s_i \quad \text{with} \quad \sum_i w_i = 1; \quad 0 \leq w_i \leq 1 \quad (1)$$

Estimates derived from each cue are prone to noise (σ_i^2). According to the MLE model, the system can reduce the noise in the combined percept by averaging different estimates (Landy et al., 1995). Noise reduction can be optimized if the cue weights w_j depend on the reliabilities ($R_j = 1/\sigma_j^2$) of the individual estimates. “Optimal” weights—resulting in the

* Corresponding author. Institute for Psychology, Gießen University, Otto-Behagel-Str. 10F, 35394 Gießen, Germany. Fax: +49 641 99 26 119.

E-mail address: Knut.Drewing@psychol.uni-giessen.de (K. Drewing).

maximal reliability of the final percept (R_p)—are proportional to the relative reliabilities of the cues (Oruç et al., 2003)¹:

$$R_p \geq R_i \forall i \text{ with } \max(R_p) \text{ for } w_j = \frac{R_j}{\sum_{i=1, \dots, j, \dots, N} R_i} \forall j \quad (2)$$

Weighted averaging (Eq. (1)) well describes the data in experiments, where two cues derived from the same physical property provide slightly conflicting information. That is, when two cues differ slightly in their magnitude information on a physical property (e.g., indicated depth in cm), weighted averaging of these magnitudes well describes perceived magnitude (measured via standard psychophysical procedures)—e.g., in within-visual integration of different depth or shape cues (Backus et al., 1999; Brenner and van Damme, 1999; Young et al., 1993). Experimental data also confirm the predictions from Eq. (2), namely a reduction of noise (measured via discrimination thresholds) in multi-cue as compared to single-cue situations (Jacobs, 1999; Perotti et al., 1998) and—for the case of visuo-haptic and visuo-auditory integration of size and location—even the predicted optimal weights (Alais and Burr, 2004; Ernst and Banks, 2002).

Although there have been many studies systematically investigating within-visual and crossmodal cue integration, there has been a surprising lack of research on cue integration within the haptic modality. Here, the case of active touch is of particular scientific interest. In active touch, observers control the movements of their fingers to gather a haptic impression of their environment. Thus, in active touch, people are able to actively pick-up the information that is most relevant. A wealth of evidence demonstrates that people can tailor their hand movements to a particular perceptual task (Flanagan and Lederman, 2001). For example, people move their hands differently when they have to judge the softness of an object as compared to its shape (Lederman and Klatzky, 1987). Such active control of informational inflow is not restricted to active touch (cf. eye movements in vision), but—as far as we are aware—active control distinguishes active touch from the situations so far examined regarding cue integration. In previous experiments—besides orienting their receptors towards the stimulus (e.g., fixating the stimulus with the foveal receptors in their eyes)—observers had negligible control on sensory inflow, thus, integrating the information that they (mostly) passively obtained. In contrast, active touch is a test case for a situation, where observers actively generate the sensory inflow from which they create their perception. The question is whether under such conditions the same combination rules apply as for passive perceptual situations. For example, in contrast to combining several cues like in the MLE model, one may speculate that active touch results in a cue selection strategy. That is, an exploration strategy that prefers one—presumably the most informative—cue, exclusively, and that takes advantage of active control by maximizing the input gathered from that cue. Such a strategy may help to overcome known capacity limitations in haptic perception, which have, e.g., shown up in poor processing of information over time and

space for shape recognition or symmetry detection (Balles-teros et al., 1998; Klatzky et al., 1991).

Consistent with the notion of cue selection, it was shown (Srinivasan and LaMotte, 1995) that cutaneous input stemming from skin deformation completely explained discrimination performance of the softness of a set of deformable surfaces, whereas kinesthetic input (i.e., information on limb posture) did not add anything. In another study (Voisin et al., 2002), however, both cutaneous and kinesthetic input contributed to performance in angle discrimination of 3D-shapes. Also, further studies revealed different influences on the active haptic perception of a single environmental property—e.g., influences of spatial surface structure and vibrations on perceived roughness (Hollins et al., 2000) or influences of friction on perceived surface orientation (Sachtler et al., 2000). However, none of these studies systematically investigated the integration of different cues into a single percept. They did not predictably manipulate the information presented by the different cues. Hence, these studies cannot reliably distinguish between different cue integration strategies.

Robles-de-la-Torre and Hayward (2001) clearly defined their cues and obtained results consistent with cue selection. They distinguished between positional and force cues for haptic shape perception: when sliding a finger across a bump on a surface, the finger follows the geometry of the bump (positional cue). At the same time, forces related to the slope of the bump act on the finger (force cue). A custom-made device provided participants position cues of a plane, a bump, or a hole (3 mm amplitude). Simultaneously, the device rendered force cues that were in conflict with the positional cues—indicating either a hole or a bump. Nearly all participants reported feeling the shape indicated by the force—not by the position—cue. The results indicate that in this case force cues clearly dominate over position cues (Robles-de-la-Torre and Hayward, 2001) and are in line with the notion of cue selection (here the force cue) for the haptic perception. However, in this experiment, a categorization task (bump, hole, or plane) was used. Such a task makes it impossible to determine whether the percepts were based on one cue only or whether one cue just influenced the percept to a higher degree than the other cue. Also, in the latter case, the percept may have been much more likely to be categorized according to the force cues—even if it was partly influenced by position cues. Put in other words, force cues may have just been weighted higher than position cues (cf. also Robles-de-la-Torre and Hayward, 2001). This latter explanation would be in accordance with the MLE model. Because the study did not quantify the percept, it is impossible to distinguish from this study between cue selection and the MLE model for cue combination during active touch.

The present study systematically investigates whether the MLE model can be used to describe cue integration during active haptic perception and, thus, whether it also applies to situations where the observer has active control over the sensory inflow (and over the perceptual cues). Therefore, we, here in Experiment 1, independently varied haptic force and position cues to curvature and quantified the percept using psychophysical methods. If active haptic perception is governed by cue selection, we would expect that the percept completely depends on one cue and is not influenced by the

¹ Given that noise distributions are Gaussian and independent from another.

other cue. If, in contrast, we find contributions of both cues to the percept and these can be described as a weighted average, this would give support to the MLE model for active haptic perception.

2. Experiment 1

We displayed our stimuli using the PHANToM haptic force-feedback device, which simulates haptic objects by monitoring the three-dimensional position of the finger-tip and applying appropriate reaction forces. That is, if the finger-tip approaches and penetrates a virtual surface, a force is calculated based on the finger's position within the virtual object. This force drives the finger out of the object, so that finger pressure applied on the virtual surface is counteracted by a reaction force of the virtual object. In the standard rendering method, the magnitude of the reaction force increases linearly with the indentation of the virtual surface by the finger tip, and the direction of the reaction force is normal to the surface. Surfaces rendered in such a manner by the PHANToM feel smooth when exploring them laterally: further, one senses the objects' stiffness when penetrating them perpendicularly (a stiffness that is limited by technical constraints of the PHANToM device). The virtual surface feels somewhat like a piece of rubber spread with liquid soap sensed through a thimble.

Here, we changed the rendering method in order to disentangle position and force cues to haptic shape (see Fig. 2): the magnitude of the force depends on how much the virtual surface is penetrated (in normal direction). Thus, the geometry of the virtual surface determined onset position and magnitude of reaction forces, and so it is providing a position cue of that surface (called position cue because it depends on finger position within the geometrically defined object). Force direction—which manifests the force cue, because it determines the forces counteracting and supporting the tangential exploratory movements—however, was manipulated separately. The directions of the reaction forces were taken from some surface with a particular curvature and projected on the virtual surface, thus providing force cue to a curvature different from that of the virtual surface. Our surfaces were rendered without any friction, in order to avoid modifications of the force direction by the participant's interaction with the object. Force direction changes tangentially to the virtual surface (=force cue), whereas force magnitude changes orthogonally to the virtual surface (=position cue). This ensures that force and position cues are always independent no matter what particular path is chosen by the user to explore the object.

We constructed a set of nine standard shapes (3D arches), while independently varying force and position cues to curvatures ($=1/\text{radius}$) of arches of 0, 8, and 16 m^{-1} . Thus, we created slight conflicts between the “force curvature” and the “position curvature”, i.e., the curvature indicated by either cue. From the percept resulting in cue conflict situations, one can estimate the cue weights in the MLE model (w_i in Eq. (1)): presuming that cue magnitudes on the stimulus level (our curvatures) correspond to values of the brain's single estimates derived from each cue (s_i in Eq. (1)), the MLE model

predicts perceived curvature to be in-between force and position curvature, whereby the relative shift of perceived curvature from force towards position curvature indicates the position cue weight and vice versa.

We quantified perceived curvature (P in Eq. (1)) of our standard shapes by measuring participants' points of subjectively equal curvature (PSE) of the standards as compared to shapes, where force and position curvatures were consistent. PSEs were determined using a two-interval forced choice task (2-IFC, “Which of two stimuli feels more convex?”) and the method of constant stimuli. That is, participants compared each standard shape repeatedly to comparison shapes of different curvature. This method can be used to derive a quantitative judgement of the standard's perceived curvature, because the same standard-comparison pairing might lead to different choices on different trials.

2.1. Materials and methods

2.1.1. Participants

Seven right-handers—naïve to the purpose of the experiment—participated for pay (average 25.7 years). Informed consent was obtained from each participant.

2.1.2. Apparatus

Participants sat in front of a visuo-haptic workbench (Fig. 1a). The workbench comprised of a PHANToM 1.5A haptic device (force feedback in the three translatory directions) and a 21" computer screen. The right index finger was connected to the PHANToM via a thimble-like holder, allowing for free movements having all six degrees of freedom in a 20-cm³ workspace. Simultaneously, the participants looked—fixated by a chin rest—via a mirror onto the screen (52-cm viewing distance). The mirror enables spatial alignment of visual with haptic display. In the present experiment, however, visual display was used only to guide participants through the experiment. A custom made software running on a PC controlled the devices and experiment, and collected responses.

2.1.3. Stimuli

The PHANToM device simulates haptic objects by applying appropriate reaction forces F_P depending on the three-dimensional finger position P . Usually, force magnitude is modeled as a spring (D = spring coefficient; i = indentation depth of finger into object) and force direction is normal to the object surface:

$$|\vec{F}_P| = D \cdot i_p \text{ and } \frac{\vec{F}_P}{|\vec{F}_P|} = \vec{n}_p. \quad (3)$$

That is, the rendering method determines how deep (in mm) the finger indents a virtual surface, and displays a force that “drives the finger out of the object” and that linearly increases with the indentation depth, here by $D = 0.5 \text{ N/mm}$ indentation. These virtual objects provide the observer with position and force cues to the object's shape that are consistent, just like corresponding cues are in real-world objects. As mentioned above, the simulated objects are frictionless and of limited stiffness.

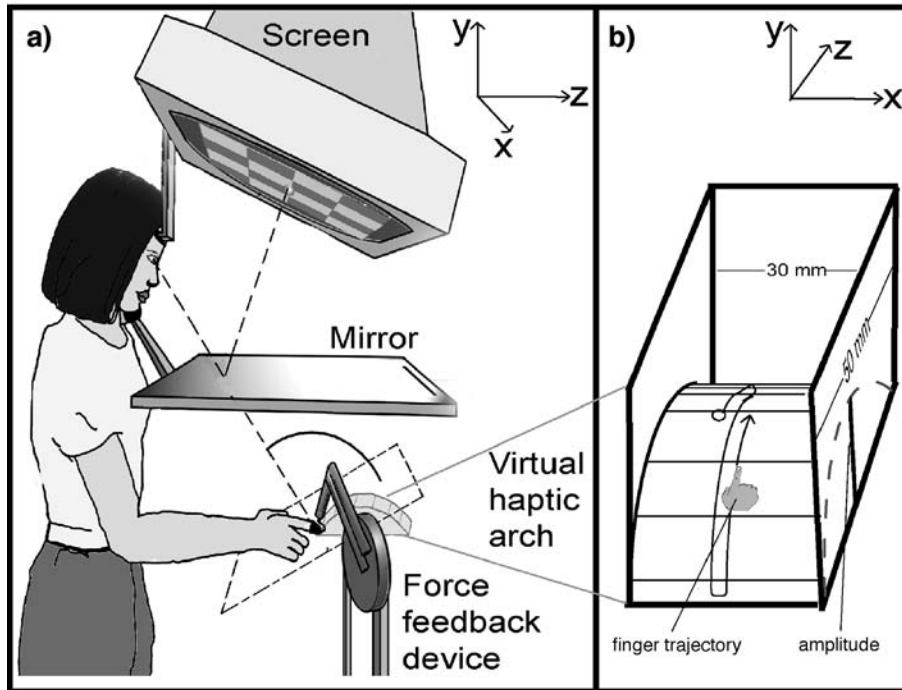


Fig. 1 – (a) Visuo-haptic workbench; note that in our experiments participants were sitting in front of the workbench instead of standing like depicted. (b) Virtual arch and movement trajectory.

However, using a force-feedback device, we can disentangle the two cues and render virtual 3D arches (sections of a circle) where the force cue determines one shape of given convexity and the position cue the convexity of another shape. For rendering the shapes, the directions of the reaction forces were determined as normals of one convex virtual surface which determines the force cue. These force directions were then projected on the geometrical surface of another convex shape which determines the position cue. The projection preserved the path distances between different force directions (see Fig. 2). Thus, the directions of reaction forces—that change tangentially to the virtual surface—create a force cue indicating one shape, whereas onset position of reaction forces and their magnitude—that changes orthogonally to the virtual surface—create a position cue to the other shape. The shapes arched in the horizontal plane along the observer's depth axis. They were touched from above and finger movement was restricted by vertical haptic walls to be within an area of 30 mm width \times 50 mm depth (see Fig. 1b).

2.1.4. Design and procedure

The design comprised two within-participant variables: *force-cue curvature* (0, 8, and 16 m^{-1}) and *position-cue curvature* (0, 8, and 16 m^{-1}) realized by nine convexly curved standard arches. We measured the points of subjective equality (PSE) and the 84%-discrimination thresholds (just noticeable difference, JND) of the standards compared to a range of arches with consistent force and position curvatures—using the method of constant stimuli in a two-interval forced choice paradigm.

Each standard was paired with 13 comparison arches, the curvature of which was equidistantly distributed in a range of $\pm 9 \text{ m}^{-1}$ around the mean value of the force and position

curvatures of the standard. Conducting 16 presentations per pair, the experiment comprised 1872 trials presented in four 2 h sessions on different days (including practice trials in the first and one break in each session). The order of trials was randomized. Each single trial consisted of the sequential presentation of standard and comparison (order balanced). Participants self-initiated the arches' presentations and, then, starting at the arch's apex made one complete stroke across each arch (forth-back-forth; Fig. 1b); the PHANTOM device blocked any further movement when the stroke was completed. Given our aim to study active exploration, we did not instruct a particular manner to move across the stimuli. However, we observed that, typically, participants' finger was in line with the direction of movement, but exerted pressure and velocity widely varied between individuals (ranges 0.9 to 3.0 N and 9.6 to 27.1 cm/s, respectively). Participants decided by a button press which of the two arches had felt more convex. Button presses were executed using the PHANTOM guided by visual buttons.

2.1.5. Data analysis

We determined individual psychometric functions for each participant and standard arch. That is, we plotted the proportion of trials in which the comparison was perceived as more convex than the standard arch against the curvature of the comparison. The PSE (point of subjective equality) is defined as the curvature of the comparison stimulus at which discrimination performance is random (here a performance of 0.5). The 84%-discrimination threshold (JND) is defined as the difference between the PSE and the curvature of the comparison when it is judged more convex than the standard 84% of the time. We obtained individual PSEs and JNDs for each

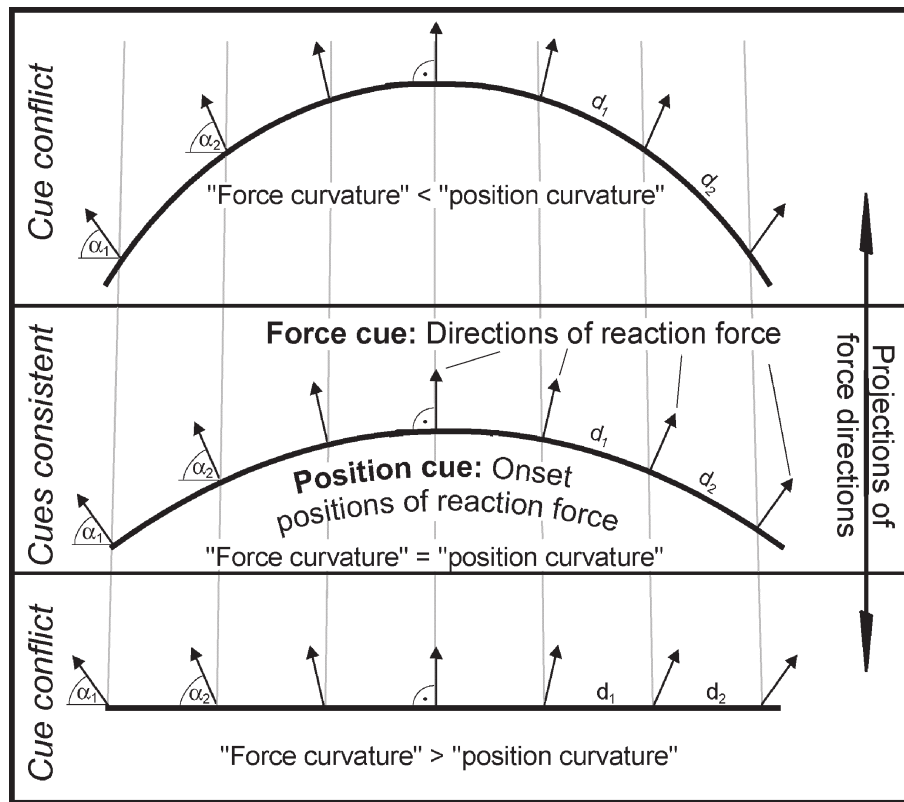


Fig. 2 – Force and position cues in arches (schematic depiction). In shapes with cue conflict, the force directions (α) of one shape were projected on the geometry of another shape, so that the path distances (d) between different force directions were preserved.

participant and standard arch from fitting cumulative Gaussians to the psychometric functions using the `psignifit` toolbox for Matlab which implements maximum-likelihood estimation methods (for details, see, Wichmann and Hill, 2001). The parameters μ and σ of the cumulative Gaussian, then, estimate PSE and JND, respectively. Individual PSEs and JNDs were the primary variables for the following analyses.

2.2. Results and discussion

On questioning after the experiment, none of the participants reported to have noticed the conflicts between the force and position cues. Individual PSEs (Fig. 3a) were entered into an ANOVA with the within-participant variables *position-cue curvature* (0, 8, 16 m^{-1}) and *force-cue curvature* (0, 8, 16 m^{-1}). Both main effects of *position-cue curvature* [$F(2,12) = 228.8$, $P < 0.001$] and *force-cue curvature* [$F(2,12) = 80.4$, $P < 0.001$] were significant, indicating that PSEs systematically increased with the increase of the curvature specified by force and position cues. Given that PSEs measure perceived curvature, the data demonstrate that both force and position cues contributed to perceived curvature. This finding does not support the notion of cue selection, but is in line with the MLE model.

We further tested whether the integration of the two cues can be described by a weighted linear combination as predicted by the MLE model—i.e., whether a weighted linear combination of force and position-cue curvature (in m^{-1} ; curvature equated with s_i in Eq. (1)) explains the PSEs (in m^{-1} ;

PSE equated with P in Eq. (1)). A marginally significant interaction *force-cue curvature* \times *position-cue curvature* [$F(4,24) = 3.6$, $P < 0.05$] points to some violation of linearity. However, a multiple linear regression (intercept = 0) of the average PSEs on the position and force-cue curvatures explained the variance between PSEs to 99%. So, deviations from linearity were minor and weighted averaging is a good approximation. We estimated the relative cue weights (w_i in Eq. (1)) by standardizing the regression coefficients, so that weights sum up to 1. The relative weight for the force cue was 46% (regression coefficient: 0.440) and for the position cue 54% (0.523).

We, additionally, calculated—separately, for each of the seven participants—multiple linear regressions of individual PSEs on the position and force-cue curvature. These regressions demonstrated at the individual level that the force and position-cue curvatures combine approximately linearly (variance explained $>94\%$ for each participant) and that position as well as force (range of force weights between individuals: 28% to 61%) contributes to perceived curvature.

Also, individual JNDs (Fig. 3b) entered into an ANOVA with the variables *position-cue curvature* and *force-cue curvature*. Both main effects of *position-cue curvature* [$F(2,12) = 20.0$, $P < 0.001^2$] and of *force-cue curvature* [$F(2,12) = 9.13$, $P < 0.02$] were significant, but not the interaction [$F < 1$ —indicating a slight

² If necessary P values corrected (Geisser and Greenhouse, 1958).

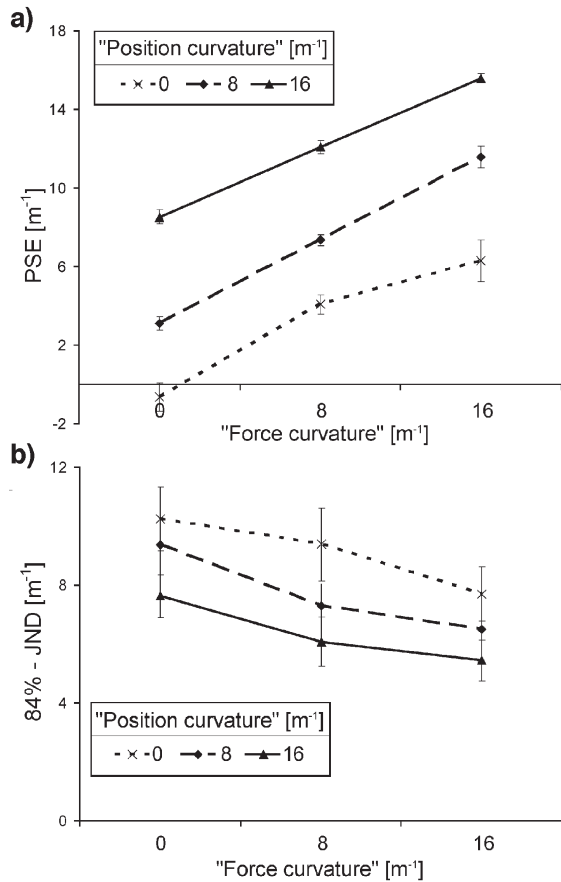


Fig. 3 – (a) Average points of subjectively equal curvature (PSE) and (b) average just noticeable differences (JND) and their standard errors as a function of curvatures indicated by force and position cues in Experiment 1.

systematical decrease of JND with increasing curvature indicated by either cue. The JNDs relate to the reliability of perceived curvature. To be more precise, the used 84%-discrimination threshold (=JND) corresponds to $\sqrt{2}$ times of the square root of the reciprocal value of reliability ($JND = \sqrt{2/R_p}$; cf. Eq. (2) and Ernst and Banks, 2002). Reliability of perceived curvature—according to the MLE model—in turn depends on the reliabilities of the single cues (Ernst and Bühlhoff, 2004). Then, from the decreases of JNDs with position-cue curvature while force-cue curvature is constant and vice versa for force-cue curvature, one can conclude that both position and force cue reliability increase with curvature. Note further that if the change in reliability is not the same for both cues, i.e., if the relation of the two reliabilities varies between the standard shapes, the MLE predicts varying cue weights (cf. Eq. (2), Hillis et al., 2002). Thus, the slight violations from a linear prediction of perceived curvature reported above may be explained by slight variations in cue weights between the standard shapes.

Overall, the results are consistent with the notion that the integration of force and position cues in haptic shape perception follows the MLE model. Our results are not in conflict with the previous report (Robles-de-la-Torre and Hayward, 2001) that the categorization of small shapes is

determined by force, but not position cues: forcing participants to categorize would result in the pattern observed in Robles-de-la-Torre and Hayward (2001), if their force cues had more than 50% weight.

Our results, however, indicate the opposite (46% force weight). But, this may be due to a couple of differences: different shapes, different exploration procedures, different rendering methods, and different haptic devices were used. Notably, in the previous experiment (Robles-de-la-Torre and Hayward, 2001), a stroke across a shape caused the finger to change with an amplitude of 3 mm. In the present experiment, the maximal amplitude was 5 mm (y in Fig. 1). Note also that the surface orientation difference within a shape (horizontal apex vs. maximal slope) in the previous experiment was about 6°. In the present experiment, it was 23° (cf. Pont et al., 1999 for the role of orientation/slope difference in curvature perception using the bare finger). Furthermore, in the present experiment, the finger’s amplitude and orientation difference within the surface, as well as cue reliabilities, changed with curvature. Maybe, it is the more pronounced finger amplitudes or the more pronounced orientation differences in the present experiment that increased relative reliability of the position cue and, thus—following the MLE model—its relative weight in comparison to the previous study. In the second experiment, we explicitly test the influences of geometric correlates of curvature on cue weight.

3. Experiment 2

Our hypothesis in Experiment 2 was that the weight of the position cues increases with a more distinct geometric variation within the shapes, i.e., a more pronounced orientation difference or a higher amplitude of the shape. We speculated that for such shapes with distinct geometric variations (here called “high” arches) the position cue is weighted relatively higher, whereas for the less convex shapes (here called “shallow” arches) the force cue becomes more dominant. Because we know from Experiment 1 that the single cues’ reliabilities for the stimuli depend on the indicated arch, such effects would be in favor of the MLE model’s prediction that the cue weights relate to their relative reliabilities (Eq. (2)).

We created two sets of virtual shapes—a “shallow” vs. a “high” arch set. Keeping the length of the shape in depth (z in Fig. 1) constant, we intermixed force and position cues indicating curvatures of 0, 5, and 10 m⁻¹ (shallow arches, amplitudes 0.0–3.2 mm, orientation differences 0–14°) and of 20, 25, and 30 m⁻¹ (high arches, amplitudes 6.7–11.3 mm, orientation differences 30–48°), respectively. Participants compared these standards to comparison shapes with consistent force and position-cue curvature. Considering the length of the experiment, we changed the method from constant stimuli (Experiment 1) to double-staircases to only determine the PSEs in Experiment 2.

3.1. Materials and methods

Apparatus, stimulus construction, and the procedure in single trials were identical to Experiment 1. The three

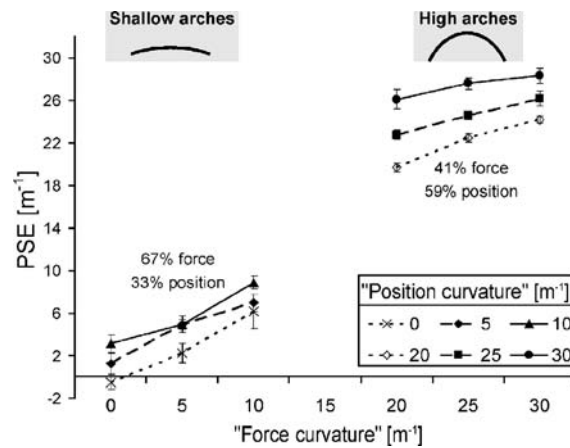


Fig. 4 – Average points of subjectively equal curvature (PSE) and their standard errors as a function of curvatures indicated by force and position cues for more convex “high” and less convex “shallow” arches in Experiment 2.

within-participant variables were *arch rise* (shallow [$x = 5 \text{ m}^{-1}$], high [$x = 25 \text{ m}^{-1}$]), *force-cue curvature* ($x - 5, x, x + 5 \text{ m}^{-1}$), and *position-cue curvature* ($x - 5, x, x + 5 \text{ m}^{-1}$) realized in 18 standard shapes.

For each standard, we conducted one double-staircase (1-up/1-down), in each of which two adaptive staircases were interleaved. In succeeding trials of both staircases, the curvature of the comparison curve was reduced by a certain step, if the participant in the previous trial of that staircase had indicated the comparison to be more convex than the standard and vice versa. In this procedure, finally, the comparison arches converge at the point of subjective equality (PSE) to the standard. Initial step sizes were 8 m^{-1} for shallow arches and 6 m^{-1} for high arches; with each reversal of step direction (and response), step size was halved—down to a smallest step size of 2 m^{-1} for shallow arches and 1.5 m^{-1} for high arches (≈ 3 reducing reversals). Each staircase stopped after 8 non-reducing reversals. From averages of the comparisons' curvatures across these 8 reversal points, we estimated the PSEs (Falmagne, 1986). The order of staircases was randomized.

The experiment lasted about 2.5 h including an initial short practice phase. We tested 14 naïve participants (right-handed; average 23.8 years) who were paid and who gave informed consent prior to the experiment.

3.2. Results and discussion

Again, none of the participants reported to have noticed the conflicts between the cues. Individual PSEs (Fig. 4) entered an ANOVA with the variables *arch rise*, *force-cue curvature*, and *position-cue curvature*. Not surprisingly, a main effect of *arch rise* [$F(1,13) = 3420.1, P < 0.001$] indicated that the more convex high arch curves were generally perceived as being more curved than the less convex shallow arches. Main effects of *position-cue curvature* [$F(2,26) = 357.1, P < 0.001$] and *force-cue curvature* [$F(2,26) = 464.5, P < 0.001$] indicated that PSEs increased with increasing curvature specified by either cue. Most importantly, the interaction of *arch rise* with *position-cue curvature* [$F(2,26) = 26.2, P < 0.01$] demonstrates

that the contribution of the position cue to perceived curvature (perceived curvature here equals the PSE) differs between the two arch sets—as does the interaction of *arch rise* with *force-cue curvature* [$F(2,26) = 39.2, P < 0.01$] for the force cue contribution. There were no other reliable effects [$F_s < 1$].

We calculated multiple regressions (intercept = 0) of the standards' PSEs on their force and position-cue curvatures separated by arch rise: for shallow arches, the relative force cue weight was 67% (regression coefficient: 0.579), the position cue weight 33% (0.281), and variance was explained to 99%; for high arches, the values were 41% force (0.401), 59% position (0.583), and 99% explained variance. The high amount of explained variance demonstrates that locally, i.e., for each arch set alone, perceived curvature can be well predicted by weighted averaging of the curvatures indicated by the two cues. Cue weights show that force cues influence the percept more in the set of the less convex shallow as compared to the more convex high arches and vice versa for position cues. This is consistent with our hypothesis that the weight of the position cues increases with geometric correlates of convexity like finger amplitude and surface orientation difference. Also consistent is the relative force cue dominance in the shallow arch set that was previously observed (Robles-de-la-Torre and Hayward, 2001).

We know from Experiment 1 that our cues' reliabilities depend on curvature. So, differences in the reliabilities between arch sets are rather probable. Thus, the observed dependency of cue weights on arch rise is consistent with the MLE model's prediction that weights depend on the cues' relative reliabilities (Ernst and Bühlhoff, 2004). We can explain our findings, then, by an increase of the relative reliability of the position cue with increasing finger amplitudes or with increasing orientation differences.

Based on this explanation, we predicted PSEs in this experiment as an alternative to the above multiple regressions. From the findings in Experiment 1, we conclude that position and force cue reliabilities systematically increase with indicated curvature. Hence, we presumed a (positive)

linear relationship between each cue's (i) reliability (R_i), and indicated curvature (C_i):

$$R_{C_i} = a_i + b_i C_i \quad a_i, b_i \geq 0 \forall i \quad (4)$$

Based on Eq. (4) and the MLE model (Eqs. (1) and (2)), we regressed the PSEs in this experiment on the curvature indicated by either cue. That is, in Eq. (1), we substituted s by C , P by the PSEs, and w by Eq. (2):

$$PSE_{C_1, C_2} = \sum_{j=1 \dots 2} (w_j C_j) = \sum_j \left(\frac{R_j}{\sum_i R_i} C_j \right) \quad (5)$$

C_1 and C_2 denote the curvatures indicated by force and position cues, respectively. Further, we substituted the reliabilities R_i by Eq. (4):

$$PSE_{C_1, C_2} = \sum_{j=1 \dots 2} \left(\frac{a_j + b_j C_j}{\sum_{i=1 \dots 2} (a_i + b_i C_i)} C_j \right) \quad \text{with } a_i, b_i \text{ const.} \quad (6)$$

Using a least-squares fit, we determined the a_i and b_i in this equation from regressing the average PSEs on the corresponding force and position-cue curvatures. Most importantly, the fit explained the variance between PSEs to 99% which is similar to the fit by multiple regressions. Note that this fit and the two multiple regressions are identical in terms of the number of free parameters (i.e., a_1, a_2, b_1, b_2 here and 2 [regressions] \times 2 [force and position] regression coefficients above). The good fit here corroborates the reliability explanation. Also consistent, the estimated slopes b_1 and b_2 were zero for the force cue and larger than zero for the position cue indicating that only position cue reliability increases with curvature, but not force cue reliability.

One interpretation of these changes in reliability is that people use particular information inherent in the cues (cf. Pont et al., 1999) that relates non-linearly to the curvature in the present shapes. Both finger amplitude or surface orientation difference may be the crucial information in the position cue. Both finger amplitude and orientation difference increase faster than the curvature (0, 3.2, 6.7, and 11.3 mm amplitude and 0, 14, 30, and 48° orientation difference correspond to the curvatures 0, 10, 20, and, 30 m⁻¹, respectively). Hence, it is reasonable that discrimination from the position cue is better for large as compared to small curvatures and that the reliability of the position cue increases with curvature. In contrast, the crucial information in the force cue might be maximal slope-related de-/acceleration. This information linearly increases with curvature and, so, should be equally reliable for all curvatures. However, our experiment was not designed to decide upon the used information and these speculations remain to be tested.

4. General discussion

In the current study, we explored whether the MLE model used to describe visual and crossmodal integration extends to cue integration during active haptic perception—by investigating the integration of force and position cues to haptically perceived shape. Experiment 1 demonstrated that

this integration can be described by a linear weighting model. This held for each individual's data in Experiment 1. Experiment 2 demonstrated that cue weights depend on the curvature of the shape. Position cue weights were higher for curvature perception of more convex high as compared to less convex shallow arches. Because we know from Experiment 1 that our cues' reliabilities relate to the particularly indicated shapes, these findings favor the assumption that cue weights depend on relative cue reliability. Thus, also within-haptic cue integration can be well described by the MLE model.

Thereby, the present study is—to our knowledge—the first systematic study on within-haptic cue integration during active exploration. The MLE model has been mostly tested under situations in that information was obtained rather "passively". Here, information is gathered under active control. For example, studies on visual depth-integration usually presented different cues statically at a single fixated position, and haptic size perception in a visuo-haptic integration study (Ernst and Banks, 2002) was limited to a single grip of one second duration. Such situations do not offer the observer much control or variation on how they obtain information. In contrast, the present study enabled participants to actively explore the stimuli and (in limits) to control the sensory inflow from which they build-up perception. One may still argue that in the present study the exploratory movements were constrained, in that participants had to do one single stroke in a prespecified manner. However, participants were able to control the movement velocity and the pressure exerted by their finger. Indeed, we observed remarkable individual variation in both pressure (range 0.9 to 3.0 N) and velocity (9.6 to 27.1 cm/s) scores³. Moreover, these movement parameters can be related to the control of the input obtained from the two cues. As to position cues, it is known that the detection threshold for finger joint rotation (=amplitude) increases with rotation velocity (Hall and McCloskey, 1983) and one may speculate that higher pressure improves the saliency of force cues (but cf. Wheat et al., 2004 on passive touch). Indeed, a multiple regression of the individual force cue weights from Experiment 1 on these movement parameters revealed a significant [$t(6) = 4.2, P < 0.02$] inverse relation of velocity and a positive (not significant) relation of pressure to force weight and explained 82% variance. These relationships and notable individual differences in cue weights (28 to 64% force) confirm that our study enabled active modulation of gathering cue information.

In conclusion, we demonstrated that cue integration in active haptic perception obeys principles formulated in the MLE model. However, there are also hints that individual movement variations can modulate integration within this framework (see also Wexler et al., 2001 for vision). It is an interesting question for future research, to determine how movement control influences cue integration and whether movement variations may be strategically exploited to optimize the input for cue integration in active perception (cf. Trommershäuser et al., 2003).

³ Averages of trial-wise 3rd quartiles of measures every 10 ms.

Acknowledgments

We thank Johannes Burge, Jean-Pierre Bresciani, Heinrich Bülthoff and five anonymous reviewers for many helpful suggestions and Sylvia Spodaru for her support in data collection. This work was supported by the 5th Framework Program of the EU (IST-2001-38040, TOUCH-HapSys).

REFERENCES

- Alais, D., Burr, D., 2004. The ventriloquist effect results from near-optimal bimodal integration. *Curr. Biol.* 14, 257–262.
- Backus, B.T., Banks, M.S., van Ee, R., Crowell, J.A., 1999. Horizontal and vertical disparity, eye position, and stereoscopic slant perception. *Vision Res.* 39, 1143–1170.
- Ballesteros, S., Millar, S., Reales, J.M., 1998. Symmetry in haptic and in visual perception. *Percept. Psychophys.* 60, 389–404.
- Brenner, E., van Damme, W.J.M., 1999. Perceived distance, shape and size. *Vision Res.* 39, 975–986.
- Bülthoff, H.H., Mallot, H.A., 1988. Integration of depth modules: stereo and shading. *J. Opt. Soc. Am. A* 5, 1749–1758.
- Ernst, M.O., Banks, M.S., 2002. Humans integrate visual and haptic information in a statistically optimal fashion. *Nature* 415, 429–433.
- Ernst, M.O., Bülthoff, H.H., 2004. Merging the senses into a robust percept. *Trends Cogn. Sci.* 8, 162–169.
- Falmagne, J.C., 1986. Psychophysical measurement and theory. In: Boff, K.R., Kaufman, L., Thomas, J.P. (Eds.), *Handbook of Perception and Human Performance*. Cogn. Process. Perform., vol. 2. John Wiley and Sons, New York, pp. 1-1–1-66.
- Flanagan, J.R., Lederman, S.J., 2001. Neurobiology—Feeling bumps and holes. *Nature* 412, 389–391.
- Geisser, S., Greenhouse, S.W., 1958. An extension of Box's results on the use of the F-distribution in multivariate analysis. *Ann. Math. Stat.* 29, 885–891.
- Hall, L.A., McCloskey, D.I., 1983. Detections of movements imposed on finger, elbow, and shoulder joints. *J. Physiol.* 335, 519–533.
- Hillis, J.M., Ernst, M.O., Banks, M.S., Landy, M.S., 2002. Combining sensory information: mandatory fusion within, but not between, senses. *Science* 298, 1627–1630.
- Hollins, M., Fox, A., Bishop, C., 2000. Imposed vibration influences perceived tactile smoothness. *Perception* 29, 1455–1465.
- Howard, I.P., Rogers, B.J., 2002. Seeing in Depth, vol. 2. Porteus, Thornhill, CDN.
- Jacobs, R.A., 1999. Optimal integration of texture and motion cues to depth. *Vision Res.* 39, 3621–3629.
- Klatzky, R.L., Lederman, S.J., Balakrishnan, J.D., 1991. Task-driven extraction of object contour by human haptics: I. *Robotica* 9, 43–51.
- Landy, M.S., Maloney, L.T., Johnston, E.B., Young, M., 1995. Measurement and modeling of depth cue combination: in defense of weak fusion. *Vision Res.* 35, 389–412.
- Lederman, S.J., Klatzky, R.L., 1987. Hand movements: a window into haptic object recognition. *Cogn. Psychol.* 19, 342–368.
- Oruç, I., Maloney, T.M., Landy, M.S., 2003. Weighted linear cue combination with possibly correlated error. *Vision Res.* 43, 2451–2468.
- Perotti, V.J., Todd, J.T., Lappin, J.S., Phillips, F., 1998. The perception of surface curvature from optical motion. *Percept. Psychophys.* 60, 377–388.
- Pont, S.C., Kappers, A.M.L., Koenderink, J.J., 1999. Similar mechanisms underlie curvature comparison by static and dynamic touch. *Percept. Psychophys.* 61, 874–894.
- Robles-de-la-Torre, G., Hayward, V., 2001. Force can overcome object geometry in the perception of shape through active touch. *Nature* 412, 445–448.
- Sachtler, W.L., Pendexter, M.R., Biggs, J., Srinivasan, M., 2000. Haptically perceived orientation of a planar surface is altered by tangential forces. Paper Presented at the Fifth Phantom User's Group Workshop. Aspen, Colorado.
- Srinivasan, M.A., LaMotte, R.H., 1995. Tactile discrimination of softness. *J. Neurophysiol.* 73, 88–101.
- Trommershäuser, J., Maloney, L.T., Landy, M.S., 2003. Statistical decision theory and the selection of rapid, goal-directed movements. *J. Opt. Soc. Am. A* 20, 1419–1433.
- Voisin, J., Lamarre, Y., Chapman, C.E., 2002. Haptic discrimination of object shape in humans: contribution of cutaneous and proprioceptive inputs. *Exp. Brain Res.* 145, 251–260.
- Wexler, M., Panerai, F., Lamouret, I., Droulez, J., 2001. Self-motion and the perception of stationary objects. *Nature* 409, 85–87.
- Wheat, E.H., Salo, L.M., Goodwin, A.W., 2004. Human ability to scale and discriminate forces typical of those occurring during grasp and manipulation. *J. Neurosci.* 24, 3394–3401.
- Wichmann, F.A., Hill, N.J., 2001. The psychometric function: I. Fitting, sampling and goodness-of-fit. *Percept. Psychophys.* 63, 1293–1313.
- Young, M.J., Landy, M.S., Maloney, L.T., 1993. A perturbation analysis of depth perception from combinations of texture and motion cues. *Vision Res.* 33, 2685–2696.